work was supported by the National Science Foundation, both through research grants and the Major Instrument program.

References and Notes

(1) S. F. Nelsen and P. J. Hintz, *J. Am. Chem. Soc.*, **94**, 7108 (1972).
(2) (a) S. F. Nelsen and J. M. Buschek, *J. Am. Chem. Soc.*, **95**, 2011 (1973); (b) S. F. Nelsen, J. M. Buschek, and P. J. Hintz, *ibid.*, **95**, 2013 (1973); (c) S. F. Nelsen and J. M. Buschek, *ibid.*, **96**, 2392 (1974); (d) *ibid.*, **96**, 6982 (1974); (e) *ibid.*, **96**, 6987 (1974).
(3) (a) P. Rademacher, *Angew. Chem.*, **85**, 410 (1973); (b) *Tetrahedron Lett.*, **83** (1974); (c) *Chem. Ber.*, **108**, 1548 (1975); (d) P. Rademacher and H. Koopman, *Chem. Ber.*, **108**, 1557 (1975).
(4) (a) S. F. Nelsen and G. R. Weisman, *J. Am. Chem. Soc.*, **96**, 7111 (1974); (b) *ibid.*, **98**, 1842 (1976); (c) *ibid.*, **98**, 3281 (1976).
(5) (a) S. F. Nelsen, P. J. Hintz, D. Olp, M. R. Fahey, and G. R. Weisman, *J. Am. Chem. Soc.*, **96**, 2916 (1974); (b) S. F. Nelsen and L. Echegoyen, *ibid.*, **97**, 4930 (1975).
(6) When θ is close to 0 or 180°, the large lone pair–lone pair interaction causes the high-energy lone-pair ionization to appear at such high energy it overlaps with σ framework ionizations. See ref 2b for an illustration of this. More seriously, it is only an approximation to call the n_+ and n_- MO's "lone pair"—there is significant mixing with the hydrocarbon portion of the molecule. Professor J. P. Snyder (Copenhagen) has pointed out to us that for *anti*-2,3-diazabicyclo[2.2.1]heptane, CNDO calculations indicate so much mixing that the two highest MO's are no longer characterizable as n_+ and n_-, but are highly localized on N(2) and N(3), respectively. We previously pointed out[2e] that the N(2),N(3) dimethyl compound gave unreasonable θ values using our $\Delta_{2,5}$ (θ) curve, and attributed this to ring strain effects. Professor Snyder's calculations indicate that mixing with the carbon framework is probably at least as important a consideration.
(7) L. L. Miller, G. C. Nordblom, and E. A. Mayeda, *J. Org. Chem.*, **37**, 916 (1972).
(8) Although the curves of Miller and co-workers[7] are labelled IP_v, they actually used adiabatic ionization potentials for at least some of the cases where the difference is significant, like amines. Either can be used for aromatics, because IP_{ad} and IP_v are numerically close.
(9) D. H. Aue, H. M. Webb, and M. T. Bowers, *J. Am. Chem. Soc.*, **97**, 4136 (1975).
(10) (a) P. A. Bischoff, J. A. Hashmall, E. Heilbronner, and V. Hornung, *Tetrahedron Lett.*, 4025 (1969); (b) E. Heilbronner and K. A. Muszkat, *J. Am. Chem. Soc.*, **92**, 3818 (1970).
(11) M. J. S. Dewar and S. D. Worley, *J. Chem. Phys.*, **50**, 654 (1969).
(12) K. Watanabe and J. R. Mottl, *J. Chem. Phys.*, **26**, 1773 (1957).
(13) V. H. Dibeler, J. E. Franklin, and R. M. Reese, *J. Am. Chem. Soc.*, **81**, 68 (1959).
(14) (a) R. W. Taft in "Steric Effects in Organic Chemistry", M. S. Newman, Ed., Wiley, New York, N.Y., 1956, Chapter 13. (b) Although σ^* has traditionally been called an inductive parameter, it would be closer to the truth to admit that the small differences between different alkyl groups are principally caused by polarizability and strain effects.
(15) (a) B. J. Cocksey, J. D. H. Eland, and C. J. Danby, *J. Chem. Soc. B*, 790 (1971). (b) For the π ionization of alkenes, μ_R values do not correlate IP_1 values well; *n*-Pr and *n*-Bu lower IP_1 even more than μ_R predicts: P. Masclet, D. Grosjean, G. Mouvier, and J. Dubois, *J. Electron Spectrosc. Relat. Phenom.*, **2**, 225 (1973).
(16) We thank Professor T. Koenig (Oregon) for first making this suggestion to us.
(17) N. Calderon, E. A. Ofstead, J. P. Ward, W. A. Judy, and K. W. Scott, *J. Am. Chem. Soc.*, **90**, 4130 (1968).
(18) F. Bartolo and F. D. Rossini, *J. Phys. Chem.*, **64**, 1685 (1960).
(19) J. D. Rockenfeller and F. D. Rossini, *J. Phys. Chem.*, **65**, 267 (1961).
(20) E. N. Peters and H. C. Brown, *J. Am. Chem. Soc.*, **95**, 2397 (1973).
(21) J. I. Brauman and L. K. Blair, *J. Am. Chem. Soc.*, **90**, 656 (1968).
(22) V. D. Parker, *J. Am. Chem. Soc.*, **96**, 5656 (1974).
(23) S. F. Nelsen, L. Echegoyen, and E. L. Clennan, unpublished data (which is an improvement, although only a 30 mV change from our previously published value: S. F. Nelsen and P. J. Hintz, *J. Am. Chem. Soc.*, **94**, 7114 (1972)).
(24) E. Eliel in "Steric Effects in Organic Chemistry", M. S. Newmann, Ed., Wiley, New York, N.Y., 1956, p 121.
(25) (a) H. C. Brown and M. Borkowski, *J. Am. Chem. Soc.*, **74**, 1894 (1952); (b) H. C. Brown and G. Ham, *ibid.*, **78**, 2735 (1956); (c) H. C. Brown and K. Ichikawa, *Tetrahedron*, **1**, 221 (1957).
(26) S. F. Nelsen and G. R. Weisman, *Tetrahedron Lett.*, 2321 (1973).
(27) S. F. Nelsen and R. T. Landis, *J. Am. Chem. Soc.*, **95**, 5422 (1973).
(28) F. E. Condon, D. C. Thakkar, and T. B. Goldstein, *Org. Prep. Proced. Int.*, **5**, 233 (1973).
(29) R. Renaud and L. C. Leitch, *Can. J. Chem.*, **32**, 545 (1954).
(30) E. Jucker and A. J. Lindenmann, patent, *Chem. Abstr.*, **64**, 3496a (1966).
(31) F. D. Green and K. E. Gilbert, *J. Org. Chem.*, **40**, 1409 (1975).
(32) H. Koch and J. Kotlan, *Monatsh. Chem.*, **97**, 1655 (1966).
(33) P. S. Engel, *J. Am. Chem. Soc.*, **91**, 6903 (1969).
(34) H. Stetter and H. Spangenberger, *Chem. Ber.*, **91**, 1982 (1958).

Electroinitiated Friedel–Crafts Transalkylations in a Room-Temperature Molten-Salt Medium[1]

V. R. Koch, L. L. Miller,*[2] and R. A. Osteryoung*[2]

Contribution from the Department of Chemistry, Colorado State University, Fort Collins, Colorado 80523. *Received December 15, 1975*

Abstract: The electrochemical oxidation of hexamethylbenzene has been studied in a room-temperature molten-salt system, namely a 67:33 mol % aluminum chloride/ethylpyridinium bromide melt and in a 50–50 by volume solution of the melt with benzene. Oxidation of hexamethylbenzene in the melt itself yielded a mixture of alkylated polyphenyl compounds and small amounts of alkylated diphenylmethanes. Preparative oxidations in the melt plus benzene yielded nearly 1 equiv each of pentamethylbenzene and diphenylmethane. The pentamethylbenzene could be oxidized further to yield tetramethylbenzene and more diphenylmethane. Coulometry, cyclic voltammetry, and ring-disk electrode studies were carried out to elucidate a mechanism for the reaction.

In recent years the organic electrochemical literature has been punctuated with reports of aluminum chloride/inorganic chloride molten-salt solvent systems.[3-8] These investigations were concerned primarily with the stability of electrogenerated intermediates and their acid–base interaction with the solvent rather than electrosynthesis per se. We had hoped to exploit the aprotic, totally anhydrous nature, and variable acid–base properties of these media to do preparative organic electrochemistry. There are, however, two experimental problems associated with these molten salts which preclude their suitability for electrosynthesis: high (for organics) liquidus temperatures and rapid homogeneous reactions with organic substrates. These problems were noted in our study of the chemical and electrochemical reactions of substituted adamantanes in $AlCl_3$/NaCl melts.[7] A recent review of organic reactions in aluminum chloride/inorganic chloride media testifies to the variety of homogeneous transformations undergone in binary and ternary melts at temperatures above 100 °C.[9] Those compounds which are stable both to the molten salt and its liquidus temperature are, in general, marginally soluble.

Molten-salt systems fluid below 50 °C are not unknown. Half-wave potentials of several organic compounds have been measured in tetrahexylammonium benzoate at room temperature.[10] Several tetraalkylammonium tetralkylborides have been synthesized[11] and the spectroscopic properties of

triethylammonium and triethylphosphonium dichlorocuprate(I) investigated.[12] Although these organic fused salts avoid the thermal and solubility problems of the aluminum chloride-based melts, they are difficult to prepare, purify, and maintain in a purified state. In addition, the benzoate and borides cannot be rendered anhydrous. While the alkylammonium cation is resistant to reduction, the anions oxidize at relatively low potentials. This severely truncates the anodic limit of the solvents, effectively prohibiting electrooxidations.[10,13]

In order to combine the best features of the aluminum chloride media and the low-temperature organic systems we have refined a room-temperature molten salt first reported by Hurley and Wier,[14] namely a 67:33 mol % aluminum chloride/ethylpyridinium bromide melt. This high Lewis-acid medium was recently shown by us to be physically and electrochemically compatible with several organometallic compounds and hexamethylbenzene.[15]

Since the melt was found to be miscible with benzene in all proportions, this study is focused on two solvent systems: the melt itself, and a 50–50 by volume solution of the melt and benzene. In this paper we elaborate upon the physiochemical properties of these solvents and describe their use as media for preparative organic electrochemistry.

Experimental Section

General. Structural determinations utilized a Perkin-Elmer Model 457 infrared spectrometer and a Varian T-60 proton magnetic resonance instrument. Gas liquid chromatographic analyses were performed on a Hewlett-Packard Model 5700 chromatograph employing a 10 ft × 0.25 in. 8% SE-30 on Chromsorb W column. Ultraviolet and visible spectra were recorded on a Cary Model 17 spectrophotometer. Melting points were measured in sealed capillary tubes by a Mel-Temp apparatus and are uncorrected.

All molten-salt experiments were conducted at 25 ± 3 °C under a prepurified nitrogen atmosphere in a Vacuum/Atmospheres Co. drybox equipped with a Model HE-493 Dri-Train. The drybox atmosphere was continuously recirculated through a column containing molecular sieves and an activated copper gettering material (BASF catalyst R3-11) which scavenged moisture and oxygen. The quality of the drybox atmosphere was such that an exposed 25-W light-bulb filament (General Electric) burned from 7 to 10 days on line voltage. This is qualitatively indicative of oxygen concentrations less than 1–5 ppm.[16]

All glassware coming in contact with the molten salt was first heated to 500 °C for several hours and then allowed to cool in the evacuated antechamber of the drybox.

Viscosities were determined using *o*-chlorophenol as a standard via the relation $y_1/y_2 = d_1t_1/d_2t_2$, where y is the viscosity, d is the density, and t is the time required for a liquid to flow through a length of tubing.

Chemicals. Hexamethylbenzene (Eastman), pentamethylbenzene, durene, and ferrocene (Aldrich) were sublimed prior to use. Diphenylmethane and fluorobenzene (Aldrich) and benzene (Fisher, spectroanalyzed) were used without further purification. Toluene was purified as per Vogel[17] and distilled just prior to use.

Ethylpyridinium bromide was prepared in 1–3 mol batches by mixing ethyl bromide (Mallinckrodt) and pyridine (Fisher), the former being in 10% excess of stoichiometric quantity. The solution was stored in the dark and allowed to react overnight. The resulting white, hygroscopic crystals were suction filtered, washed with anhydrous ethyl ether, and immediately transferred to a vacuum desiccator. Traces of the wash solvent were removed under vacuum. A dish of magnesium perchlorate was then placed inside the desiccator and the system maintained in vacuo for a minimum of 24 h. During this period the desiccator was occasionally brought to atmospheric pressure with dry nitrogen, opened, and both the pyridinium salt and magnesium perchlorate stirred. After drying, the salt was brought into the drybox and stored in a tightly capped jar. This procedure afforded ethylpyridinium bromide, mp 118–119 °C (lit.[18] mp 114 °C).

Melt Preparation and Purification. Ethylpyridinium bromide (1 gram formula weight) was weighed out and added to a Pyrex cell, the description of which may be found elsewhere.[19] When 2 gram formula weights of aluminum chloride (Fluka, A. G., anhydrous and iron free) were carefully added to the pyridinium salt, a spontaneous, exothermic reaction took place, resulting in a clear, gold-colored solution.[20] Though fluid at room temperature, the melt was placed in a furnace[19] thermostatted at 80 °C to expedite purification by galvanostatic electrolysis.

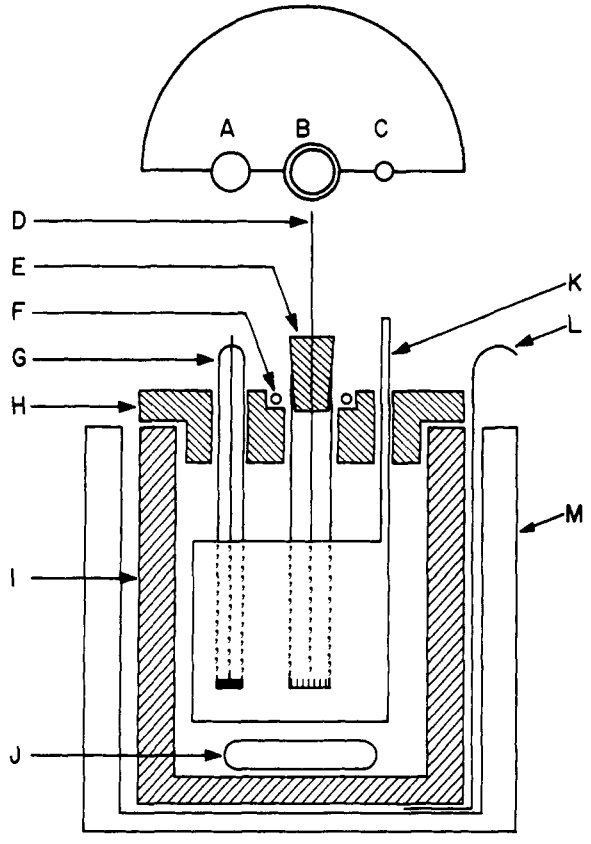

Figure 1. Preparative electrochemical cell: A, 10-mm hole for analytical working electrode; B, 12-mm hole for fritted reference compartment; C, 4-mm hole for cathode; D, Al reference electrode; E, Teflon stopper; F, O-ring; G, analytical working electrode; H, Teflon cell top; I, preparative working electrode; J, Teflon spin bar; K, Al counter electrode; L, Al foil contact; M, Pyrex beaker.

An aluminum anode rod (0.25 in. diameter, Johnson Matthey Chemicals, specpure) and a coiled aluminum wire cathode (23 mil, Alfa m5N) were introduced into the melt and electrolysis was initiated by a Kepco Model KRS-M voltage-regulated power supply (anodic current density ~0.6 mA cm^{-2}). After several hours of electrolysis, gray, pulverulent aluminum dendrites appeared on the cathode. Within 48 h shiny, leaf-like dendrites were observed to form and continued to grow throughout the electrolysis. This procedure was continued for 14–21 days, after which the gold color completely disappeared yielding a clear, water-white melt. The aluminum anode rod was cratered and covered with an oily black film. No film appeared on a clean aluminum rod introduced into the purified melt, nor did one result from subsequent electrolysis. The melt remained clear and colorless in the drybox at 25° for several weeks, after which it began to turn slightly yellow. Further electrolysis restored the melt to a colorless condition. When brought out of the drybox the melt turned dark brown within minutes.

The densities of the melt and 50–50 by volume melt–benzene were found to be 1.51 and 1.26 g/ml, respectively.

Cell and Electrodes. Preparative oxidations were performed in an undivided cell (Figure 1) employing either a 50 × 50 mm vitreous carbon crucible (Atomergic Chemicals, V25 grade) or a 3 × 1.5 in. tungsten crucible (ROC/RIC) as working electrodes. Counter electrodes were fashioned from aluminum foil (10 mil, Alfa m5N). The reference electrode for all experiments was a coiled aluminum wire (23 mil, Alfa, m5N) separated from the working and counter electrodes by a fine glass frit.

The electroanalytical data were obtained at two disk working electrodes isolated in fritted compartments: a 2.7-mm diameter vitreous carbon rod (Atomergic Chemicals, V10 or V25 grade) sealed in Pyrex,[21] and a ⅛ in. diameter tungsten rod (Alfa, m3N8) sealed

into Pyrex with a bead of uranium glass. The tungsten disk was exposed by grinding on a carborundum belt and polished on a glass plate with a slurry made from 600 grit silicon carbide powder and water. Both the tungsten and vitreous carbon electrodes were then buffed to an ultrasmooth, mirror-like surface on a polishing wheel with 0.1 μm aluminum (Fisher, Type B) and water. The geometrical area of these electrode surfaces was used in all electrochemical calculations. The electrodes were rinsed with acetone, then distilled water, and dried in an oven prior to introduction into the drybox. These procedures provided highly reproducible surfaces.

The conductivity study employed two parallel 1-cm^2 aluminum electrodes cut from foil (10 mil, Alfa, m5N). The cell constant was determined by measuring the conductivity of an aqueous 0.1 M LiCl solution.

Electrochemical Instrumentation. Cyclic voltammograms and chronoamperometric *IT* curves were recorded with either a PAR (Princeton Applied Research) Model 170 electrochemistry system or a multipurpose instrument[22] coupled to a Hewlett-Packard Model 7030 A *X-Y* recorder. *IR* compensation was used in conjunction with rapid-scan cyclic voltammograms which were recorded on a Tektronix Model 564 oscilloscope with Type 3A3 and Type 2A63 plug-in modules. Oscilloscope traces were photographed with a Tektronix Type C12 Polaroid camera.

Conductivity measurements were made with a Hewlett-Packard Model 4260A universal bridge set at 1 kHz.

Double potential step chronoamperometry was performed with a PAR Model 173 potentiostat/galvanostat equipped with a PAR Model 179 digital coulometer. The analog current output compensated for *IR* drop was interfaced with Digital Equipment Corp. Models PDP-12 and PDP-8/e computers. Data obtained by the computers were recorded on a Hewlett-Packard Model 7034 A *X-Y* recorder with point plotting capabilities.

Normal pulse voltammograms were obtained with a PAR Model 174 Polarographic Analyzer.

Constant potential preparative electrolyses were performed with either a PAR Model 173 potentiostat/galvanostat equipped with a PAR Model 179 digital coulometer or a Wenking Model 61 RS potentiostat. An Acromag Model 212-LX-1 current integrator was used in conjunction with the Wenking potentiostat for coulometric measurements. Potentials were measured and instruments calibrated with a Keithley Model 168 autoranging digital multimeter.

Rotating-Disk and Ring-Disk Experiments. All rotating-disk and ring-disk studies were conducted with a model ASR rotator (Pine Instrument Co.). The vitreous carbon ring-disk electrode employed in this study was fabricated in these laboratories and will be the subject of a forthcoming publication.[23] A bipotentiostat based on circuitry described by Bruckenstein and co-workers[24] afforded independent potentiostatic control of the ring and the disk. When the disk was potentiostated on a diffusion-limited plateau and the ring scanned, no change in disk current was observed. This indicated that there is no electronic interaction between the ring and the disk due to uncompensated *IR* drop. The disk and the ring currents were recorded on a Houston Instruments Model 2000 *X-Y* recorder in successive sweeps.

Preparative Electrolyses. Weighed amounts of hexamethylbenzene (HMB) or pentamethylbenzene (PMB) were brought into the drybox in screw-cap vials as were the aromatic cosolvents. From 15 to 25 ml of melt was pipetted into the reaction vessel. An equivalent volume of cosolvent was then added, yielding a slightly yellow solution. A background cyclic voltammogram using an analytical working electrode and steady-state currents using the crucible as the working electrode were recorded. When the HMB or PMB was brought into solution via a magnetic stirrer and Teflon spin bar, a bright yellow solution resulted. Another cyclic voltammogram was recorded, after which electrolysis commenced. During the course of the oxidation, electrolysis was momentarily discontinued to allow cyclic voltammograms to be recorded.

When an oxidation was completed, the cell was brought out of the drybox and the contents *carefully* poured over ice in a fume hood. The aqueous layer was twice extracted with 100 ml of ether and the combined organic fractions washed with three 200-ml portions of water to remove any remaining salts. After drying over magnesium sulfate, the ether and cosolvent were removed on a rotary evaporator. Traces of solvent were carefully evaporated, after which the reaction products were weighed and analyzed by GLC. Products were collected by preparative GLC and their infrared and ^{1}H NMR spectra compared to the spectra of authentic samples or to published spectra. Product distributions as determined by GLC peak areas were corrected for the thermal response of each constituent.

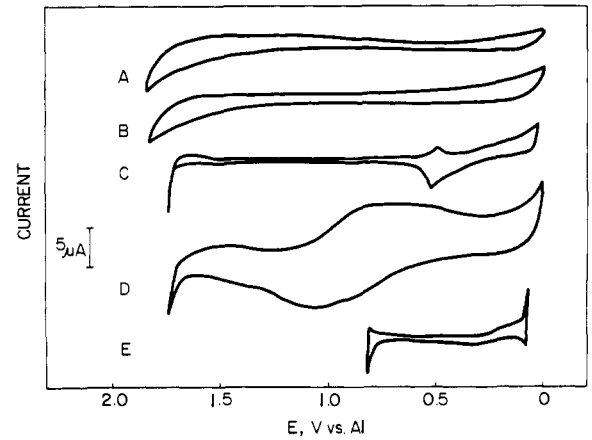

Figure 2. Cyclic voltammograms of background of working electrode materials in 2:1 aluminum chloride/ethylpyridinium bromide: A, 0.057-cm^2 vitreous carbon; B, 0.078-cm^2 tungsten; C, ~0.001-cm^2 gold; D, ~0.001-cm^2 platinum; E, ~0.03-cm^2 hanging mercury drop. Sweep rate = 0.2 V/s.

Results and Discussion

Background Processes. Several working electrode materials were investigated using the melt and the melt plus benzene. All potentials are referenced with respect to the Al^{3+}/Al^0 couple. The voltammograms were identical for each medium and are shown in Figure 2. Vitreous carbon and tungsten have the widest potential range accompanied by the lowest current density. Gold and platinum yielded large current densities and appear to react with the media in that further cycling resulted in new oxidation/reduction waves which grew with time. While the hanging mercury drop is inert to these media, its anodic potential range is limited by mercury oxidation. Thus, vitreous carbon and tungsten were used interchangeably in either the melt or the melt plus benzene.

The cathodic limit occurs at the onset of aluminum deposition (−0.2 V) on both working electrodes. In a purified melt the anodic limit was shown to be related to the formation of bromine at 1.9 V. When either vitreous carbon or tungsten was cycled into background, the reverse sweep revealed a broad irreversible reduction wave, E_p = 1.1 V. A reduction wave at this potential could be produced synthetically by adding a drop of bromine to the solvent and cycling between the background limits. Benzene is electrochemically inert over the available potential range.

Physical Properties. The ferrocene–ferricinium ion couple was previously shown to be chemically stable to and electrochemically reversible in the melt.[14] Normal pulse voltammetry (Figure 3) was employed to determine the diffusion coefficients of ferrocene in the melt and the melt plus benzene. Both curves manifest a simple one-electron reversible process. Plots of log $(i_d - i/i)$ vs. E were linear with slopes of 60 mV and $E_{1/2}$ values of 0.25 V.

Since the viscosity of the melt decreases with the addition of benzene, one would expect the diffusion coefficient of an electroactive species to increase. This is borne out by Figure 3. Though the concentration of ferrocene is halved in the melt plus benzene, the limiting diffusion current is almost 90% of that in the melt alone. These data are tabulated in Table I and compared to published values for the viscosity of acetonitrile and the diffusion coefficient of ferrocene in acetonitrile, a common solvent for preparative organic electrochemistry.

Another desirable physical property for electrochemical applications is a high specific conductance, κ_{sp}. As shown in

Table I. Physical Properties at 25 °C

Solvent system	N^a	$D \times 10^{7\,b}$	$\kappa_{sp} \times 10^{3\,c}$
Melt	24.8	4.1	16.9
50–50 melt–benzene	4.9	11.6	33.9
Acetonitrile, 0.2 M $LiClO_4$	0.34[d]	240.0[e]	7.1

[a] Viscosity in centipoises. [b] Diffusion coefficient of ferrocene in $cm^2\ s^{-1}$. [c] Specific conductivity in $(ohm\ cm)^{-1}$. [d] R. C. Weast, Ed., "Handbook of Chemistry and Physics", 51st ed, Chemical Rubber Publishing Co., Cleveland, Ohio, 1970–1971, p F-37. [e] T. Kuwana, D. E. Bublitz, and G. Hoh, *J. Am. Chem. Soc.*, **82**, 5811 (1960).

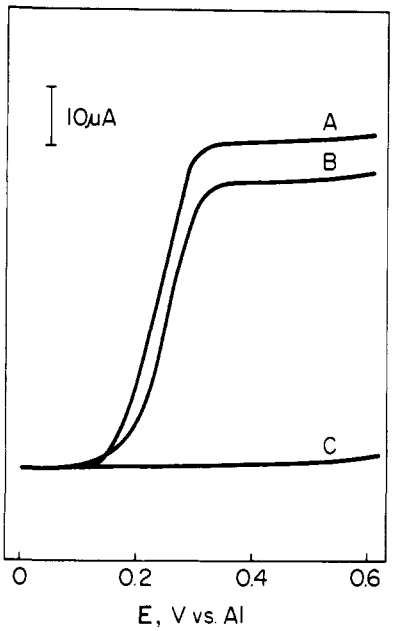

Figure 3. Normal pulse voltammograms at vitreous carbon: A, 6 mM ferrocene in melt; B, 3 mM ferrocene in melt plus benzene; C, background. Sweep rate = 2 mV/s; 1 pulse/s.

Table I the specific conductance doubles in going from the melt to the melt plus benzene, presumably due to increased ionic mobility in the less viscous medium. The specific conductance of the melt plus benzene is seen to be appreciably larger than the acetonitrile/lithium perchlorate system.

While both the melt and melt plus benzene are suitable solvents for visible spectroscopy[15] the optical windows in the ultraviolet region cut off at 288 and 320 nm, respectively.

Cyclic Voltammetry of Alkylaromatic Compounds. Cyclic voltammograms of hexamethylbenzene (HMB) at tungsten (Figure 4) and vitreous carbon were recorded in the melt and melt plus benzene. Starting from the rest potential and sweeping initially in a cathodic direction, all four voltammograms yielded an irreversible anodic wave (E_p = 1.35 V) corresponding to the oxidation of HMB. After passing through the anodic wave, the second cathodic sweep revealed differentiations in the number and peak potentials of reduction waves depending upon solvent and electrode material.

At a tungsten electrode in the melt a broad, ill-defined cathodic wave from 0.5 to 0.1 V is observed along with another cathodic wave, E_p = −0.1 V. In the melt plus benzene, however, only the more cathodic wave appears. At vitreous carbon in the melt, a cathodic wave, E_p = 0.15 V, appears after the first anodic sweep. No reduction wave at −0.2 V is evident, only an increase in cathodic current. In the melt plus benzene the wave at 0.15 V disappears while the increased current at −0.2 V remains. Clearly, all of the cathodic waves are a consequence of HMB oxidation as they are absent in the initial cathodic sweep.

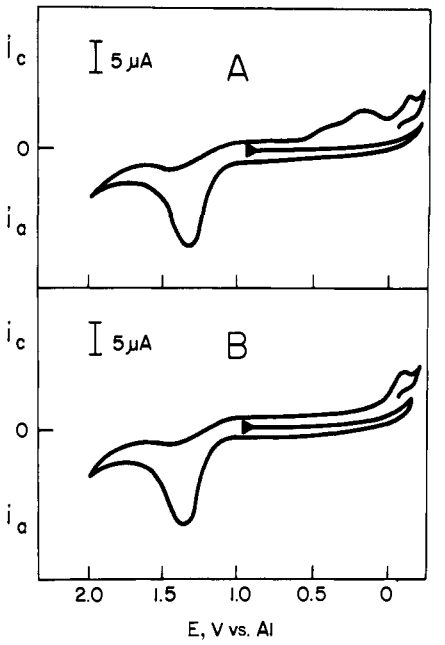

Figure 4. Cyclic voltammograms at tungsten: A, 5.7 mM HMB in melt; B, 2.85 mM HMB in melt plus benzene. Sweep rate = 0.2 V/s.

An earlier paper[15] suggested that the wave at 0.15 V on vitreous carbon in the melt was due to the reduction of proton to hydrogen. In fact, proton reduces at more negative potentials. When hydrogen chloride gas is bubbled through either the melt or melt plus benzene, a reduction wave (E_p = −0.1 V) is observed at tungsten while the foot of a reduction wave is seen at vitreous carbon. In both molten-salt media at either electrode, the oxidation of hexamethylbenzene involves the generation of proton.

Cyclic voltammograms of HMB were recorded for several concentrations and sweep rates in the melt and melt plus benzene. Plots of peak current vs. HMB concentrations of from 3–13 mM were linear, indicating a first-order dependence on HMB. Plots of peak current vs. the square root of the sweep rate from 0.5–1.0 V/s were also linear, indicating that the electron transfer step is diffusion controlled. These data are consistent with a process in which HMB simply diffuses to the electrode and gives up an electron.

At scan rates less than 10 V/s, cyclic voltammograms of HMB oxidation are completely irreversible. Beyond 10 V/s, however, some reverse current is observed. Figure 5 depicts first sweep voltammograms of HMB at 50 V/s at a tungsten electrode in both media. Results at carbon electrodes were similar. The addition of benzene to the melt results in more reverse current at either working electrode. The anodic and cathodic peak separations are about 80 mV, 60 mV being the theoretical value for a one-electron reversible redox couple at 25 °C. Thus, at very fast sweep rates the HMB cation radical ($HMB^{\cdot+}$) can be reduced prior to undergoing a rapid chemical follow-up reaction. While $HMB^{\cdot+}$ has been detected at −70 °C in methylene chloride,[25] there have been no reports of its existence at room temperature. Indeed, in trifluoroacetic acid, a solvent touted for its cation radical stabilizing ability, $HMB^{\cdot+}$, escaped detection.[26] Our results in the room-temperature molten-salt media support previous work[4-6] ascribing the unusual cation radical stability to the nonnucleophilic nature of aluminum chloride based molten salts.

At 50 V/s the reduction waves at 0.2 V were still evident in the melt while absent in the melt plus benzene. Due to large charging currents and the proximity to aluminum deposition, the presence or absence of proton reduction could not be ascertained.

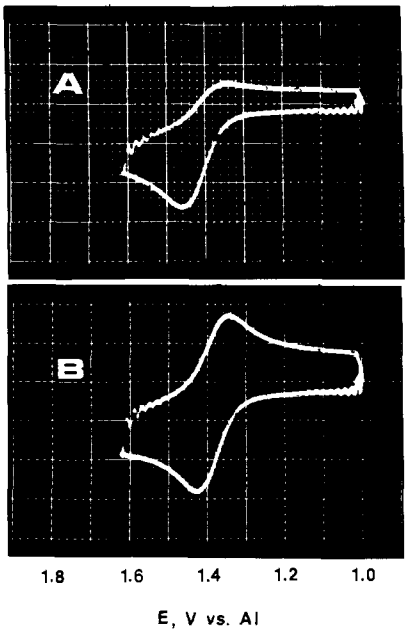

Figure 5. Cyclic voltammograms at tungsten: A, 6.4 mM HMB in melt; B, 3.2 mM HMB in melt plus benzene. Sweep rate = 50 V/s. Each large division = 200 μA.

Alkylaromatic homologues of HMB such as pentamethylbenzene (PMB) and durene (TMB) manifest voltammetric behavior similar to that of HMB. While the oxidative peak potentials of PMB and TMB are shifted to more anodic values, the kinds of positions of reduction waves as a function of electrode material and solvent are the same as reported for HMB.

These data are summarized in Table II and are compared with literature values for the oxidation of these alkylaromatics and ferrocene in acetonitrile. The half-wave or $E_{p/2}$ potentials in the molten-salt system are shifted in the anodic direction by about 180 mV compared to those in acetonitrile. Peaks for tetramethylbenzene (TMB) and diphenylmethane (DPM) oxidation were not observed prior to bromine discharge.

The potentiostatic oxidation of HMB was performed using both tungsten and vitreous carbon crucible electrodes at 25°. The solubility of HMB in the melt and melt plus benzene was found to be 2.6 g/100 ml and 3.1 g/100 ml, respectively.

Initially HMB concentrations ranged from 20 to 45 mM; initial currents at 40 mM were typically a factor of 200 larger than the background; e.g., 60 mA vs. 0.3 mA at +1.60 V. The current was observed to decay exponentially with time as an oxidation proceeded.

HMB oxidations in the melt itself yielded a tarry, yellow-brown material. GLC analysis revealed a variety of closely eluting, high-boiling components. Infrared and ^{1}H NMR spectroscopy indicated a mixture of alkylated polyphenyl compounds and small amounts of alkylated diphenylmethanes. No chlorinated or brominated species were detected on the basis of spectroscopy and a negative Beilstein test for halogens. These results are in qualitative agreement with earlier work regarding the electrochemical oxidations of polymethylbenzenes in other solvents of low nucleophilicity.[27,28] In either nitromethane or methylene chloride the anodic oxidation of alkylaromatics afforded mixtures of methylated biphenyls, diphenylmethanes, and substantial amounts of polymer.[29]

Preparative electrooxidations undertaken in the 50–50 by volume melt–benzene and in other 50–50 melt–aromatics produced simpler results as shown in Table III. When 1 equiv of HMB was potentiostatically oxidized at 1.30 V, at either tungsten or vitreous carbon, 1 equiv each of PMB and diphenylmethane (DPM) was formed

Table II. Voltammetric Data

Substrate, 5 mM	Solvent: Acetonitrile $E_{p/2}$,[a] V	Solvent: 50–50 melt–benzene $E_{p/2}$,[b] V
Ferrocene	0.06	0.25
HMB	1.16	1.30
PMB	1.28	1.46
TMB[c]	1.50	
DPM	1.82[d]	

[a] $E_{p/2}$ vs. 0.1 M Ag^+/Ag at Pt, from N. L. Weinberg and H. R. Weinberg, *Chem. Rev.*, **68**, 449 (1968). [b] $E_{p/2}$ vs. Al, 0.2 V/s at W or C. [c] 1,2,3,5-Tetramethylbenzene. [d] Measured by V. R. Koch.

$$HMB + 2C_6H_6 \rightarrow PMB + DPM + 2H^+ + 2e^- \quad (1)$$

Coulometry indicates that two electrons are transferred per molecule of substrate. By adjusting the applied potential to more anodic values, one product of the reaction, PMB, could be further oxidized to give tetramethylbenzene (TMB) and a second mole of DPM. While the amounts of isolated TMB are low at higher potentials, the conversion of HMB to PMB is quite high. Thus, the kinds and relative amounts of products are intimately dependent upon the applied potential. As seen in Table II, DPM is electrochemically inert to these potentials and accrues at the expense of the polymethylbenzenes.

These data are shown to be internally consistent by the preparative oxidation of PMB. Thus, PMB is converted to TMB and DPM; since TMB is just anodically accessible it too can be oxidized to a trimethylbenzene and DPM as shown

$$PMB + 2C_6H_6 \rightarrow TMB + DPM + 2H^+ + 2e^- \quad (2)$$

$$TMB + 2C_6H_6 \rightarrow TriMB + DPM + 2H^+ + 2e^- \quad (3)$$

GLC analysis of these product mixtures revealed the TMB fractions to be composed of two isomers. The major component (95% of the total) was collected and identified as 1,2,3,5-tetramethylbenzene (isodurene). While the trimethylbenzene was not GC collected it was shown to have the same retention time as 1,3,5-trimethylbenzene (mesitylene).

Hexamethylbenzene was also oxidized in the presence of other aromatic cosolvents as seen in Table III. With toluene a mixture of three diphenylmethanes was observed on the GC trace in ratios of 55:37:8. These presumably correspond to the *p,p'*-, *o,p'*-, and *o,o'*-dimethyldiphenylmethanes. When fluorobenzene was used as the cosolvent, one broad diphenylmethane peak was observed. The NMR spectrum, however, revealed a variety of difluorodiphenylmethanes to be present.

Control experiments demonstrated that demethylation of HMB and formation of DPM were electrochemically initiated. Hexamethylbenzene was stirred overnight in the cell containing melt plus benzene. Upon workup, a 97% recovery of HMB was achieved. This experiment was repeated in the presence of proton introduced as HCl gas. After workup, 99% of the added HMB was recovered unchanged. That the intermediates leading to PMB and DPM are short-lived was shown by oxidizing HMB in the melt and then adding an equal volume of benzene. Only the usual tarry material was obtained.

Mechanistic Aspects. Preparative oxidation of HMB in the melt plus benzene at potentials near 1.3 V gave only PMB and DPM as organic products in high material and coulombic yield. The following discussion is therefore directed to the reaction under these conditions.

Our premise is that HMB is the source of the central

Table III. Alkylaromatic Oxidation Products in 50–50 Melt–Cosolvent at 25 °C

Substrate	Cosolvent	Anode potential, V[a]	Consumed substrate, mmol	n[b]	Products, mmol			% current yield[c]		% product yield[d]	
					TMB	PMB	DPM	$ArCH_3$	DPM	$ArCH_3$	DPM
HMB	Benzene	1.30	0.75	1.6		0.53	0.58	66	73	71	77
HMB	Benzene	1.35	0.95	2.0		0.74	0.84	74	84	78	88
HMB	Benzene	1.60	1.48	4.5	0.78	0.30	2.11	38	94	39	142
HMB	Toluene	1.55	1.58	3.9	0.19	0.79	2.17	60	111	62	137
HMB	Fluorobenzene	1.60	1.00	2.5	0.13	0.64	1.19	72	95	77	119
					Tri MB	TMB	DPM				
PMB	Benzene	1.55	0.96	2.3	0.04	0.68	1.10	66	96	75	114

[a] At vitreous carbon vs. Al. No variation in products or distribution was noted at tungsten. [b] n faradays of electricity consumed. [c] Assuming the oxidation of $ArCH_3 \rightarrow$ DPM required 2 mF/mmol. $ArCH_3$ represents the sum of isolated methylbenzenes, e.g., $(4TMB + 2PMB)/n$. [d] Based on the amount of isolated $ArCH_3$ and DPM compared to consumed substrate.

methylene of DPM leaving PMB, and that the benzene cosolvent is the source of the two phenyl groups in DPM. A series of reversible Friedel–Crafts alkylations and transalkylations can lead logically to these products if the formation of a pentamethylbenzyl cation is postulated.

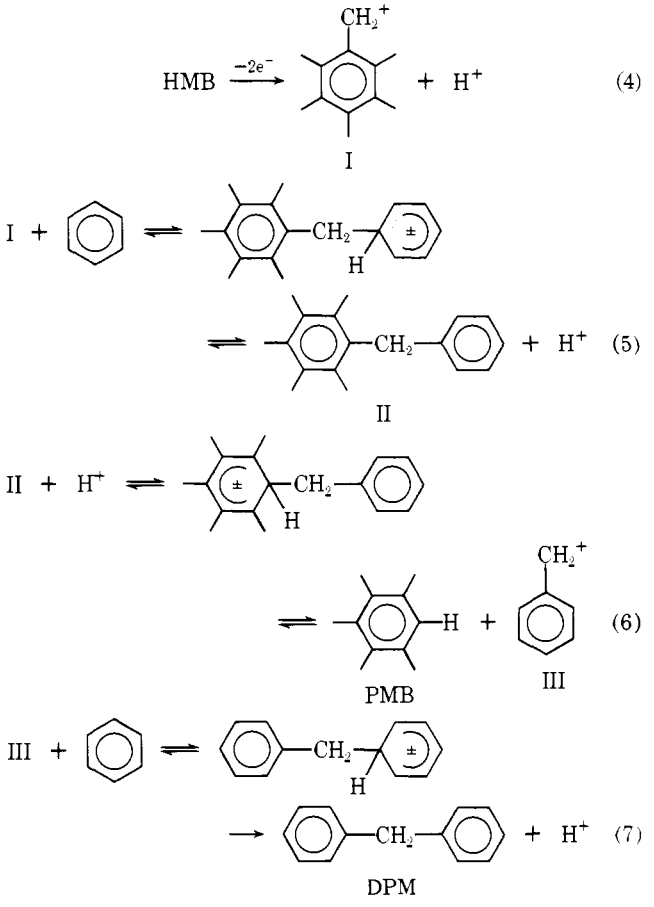

These kinds of reactions in Lewis-acid media are well documented.[30-32] Indeed, a recent report has shown that electrochemically generated pentamethylbenzyl cation reacts in the presence of benzene, dichloromethane, and trifluoroacetic acid to yield PMB and DPM.[33]

This mechanism indicates that 2 e/molecule are required overall, in agreement with the observed coulometry. We have obtained evidence, however, which strongly suggests that the above mechanism is incomplete. Not only is there evidence for a rather unstable $HMB^{\cdot+}$, but also another metastable intermediate formed by a one-electron oxidation.

Consider first the cyclic voltammetry data at the fastest sweep rates. As shown above these data indicate reversible formation of $HMB^{\cdot+}$. This must be a one-electron process and by comparison of the peak heights of ferrocene (a known one-electron reversible system) and HMB, it is concluded that their diffusion coefficients are very similar.

Another approach to n-value determinations independent of diffusion coefficients involves two electroanalytical experiments on one substrate/solvent system: cyclic voltammetry and chronoamperometry. By dividing the Randles–Sevcik equation by the Cottrell equation, an expression (eq 9) relating n to readily measured parameters is obtained, i.e.,

$$\frac{n^{3/2}}{n} = \frac{\dfrac{i_p}{2.98 \times 10^5 AD^{1/2}Cv^{1/2}}}{\dfrac{it^{1/2}}{5.45 \times 10^4 AD^{1/2}C}} \tag{8}$$

$$n^{1/2} = 0.18\left(\frac{i_p}{v^{1/2}}\right)\left(\frac{1}{it^{1/2}}\right) \tag{9}$$

Thus, n values can be calculated from the measured peak current at a given sweep rate (cyclic voltammetry), and the current–time dependence (chronoamperometry). Experimental n values for HMB in the melt and in the melt plus benzene at either tungsten or vitreous carbon ranged from 0.80 to 0.99. Though the oxidation of HMB is irreversible at slow sweep rates, the electron transfer itself is fast and can be made reversible on going to sufficiently fast sweep rates. According, we feel justified in using $n^{3/2}$ rather than $n(\alpha n)^{1/2}$ in the Randles–Sevcik equation.

At slow sweep rates the cyclic voltammograms show that $HMB^{\cdot+}$ is no longer present on cycling back. The data indicate a lifetime for $HMB^{\cdot+}$ on the order of several milliseconds. Of particular interest, however, is the observation that no peak corresponding to PMB oxidation is present in these voltammograms, indicating that it is not yet formed and that some metastable intermediate intercedes between $HMB^{\cdot+}$ and PMB (eq 10 and 11). It should be noted that the PMB wave could be detected by cyclic voltammetry during preparative oxidations of HMB or by adding PMB to the HMB solution used for cyclic voltammetry.

$$HMB \rightleftharpoons HMB^{\cdot+} \rightarrow \text{“x”} \tag{10}$$

$$\text{“x”} \rightarrow PMB + DPM \tag{11}$$

The oxidation state of the metastable intermediate “x” can be elucidated from cyclic voltammetry, rotating disk, and double potential step chronoamperometric experiments.

It is first noted that a plot of HMB peak currents vs. the

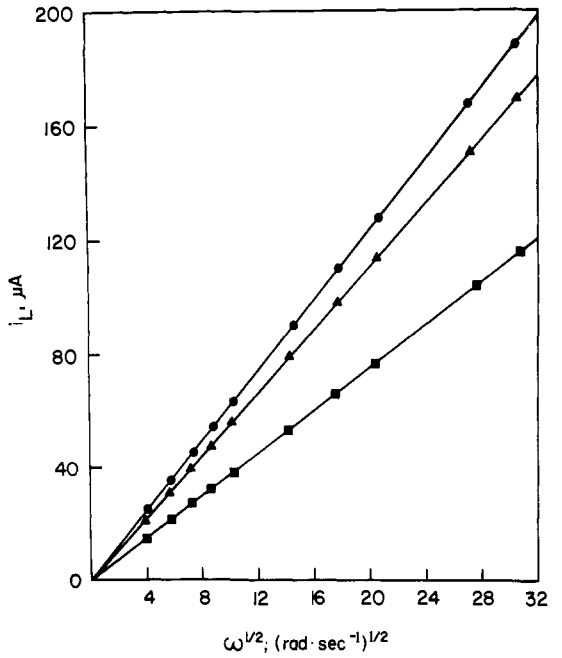

Figure 6. Steady-state Levich plots at vitreous carbon RRDE: (●) = 8.0 mM ferrocene in the melt; (▲) = 6.5 mM HMB in the melt; (■) = 2.6 mM HMB in the melt plus benzene. Limiting currents measured at 0.6 V for ferrocene and 1.6 V for HMB.

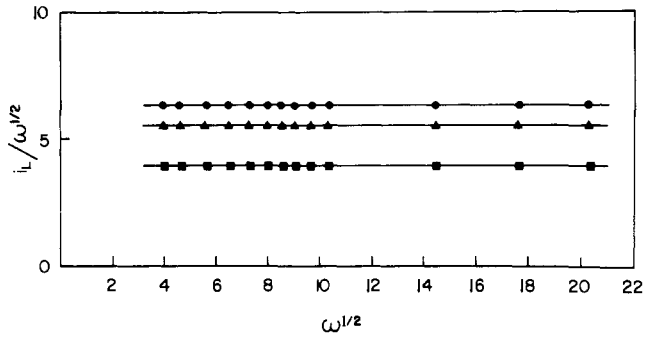

Figure 7. Limiting current plots at vitreous carbon RRDE. Same conditions as in Figure 6.

Table IV. Kinetic Data from Double Potential Step Chronoamperometry

% benzene[a]	k, s^{-1} [b]	$t_{1/2}$, ms[c]
0	67	10
25	50	13
50	26	26
75	17	40
100	12	57
150	8	83
300	6	114

[a] Amount of benzene added to melt. [b] Pseudo-first-order decomposition rates for HMB·$^+$. [c] Half-life of HMB·$^+$.

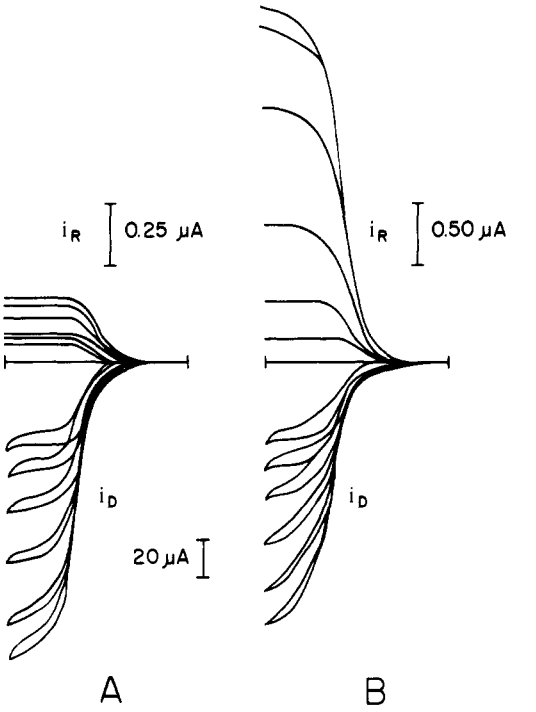

Figure 8. Comparison of ring and disk currents at ω values of 500, 1000, 2000, 4000, 7000, and 9000 rpm: A, 6.5 mM HMB in melt; B, 3.25 mM HMB in melt plus benzene. Scan rate = 20 mV/s from 1.0 to 1.6 V.

square root of the sweep rate is linear, indicating that intermediate "x" is at the one-electron stage even though HMB·$^+$ has reacted. The usual observation is a change in slope from one-electron to two-electron reactions when an initial cation radical is unstable at slow sweep rates.

Levich plots (Figure 6) of diffusion currents vs. rotation speed for ferrocene, HMB in the melt, and HMB in the melt plus benzene are linear and extrapolate to zero. Were the usual ECE process operative, one might expect to see a two-electron transfer at low ω values and a one-electron transfer at high rotation rates. This is contingent upon a fast chemical follow-up reaction and a second electron transfer observable at low rotation rates. If the disk electrode can be rotated fast enough, the electroactive product generated by the chemical step will be swept into the bulk solution prior to undergoing a second electron transfer. Since the slope of the Levich plot incorporates n, nonlinear behavior for an ECE mechanism would be expected. In fact, no change in slope for HMB in either medium was observed.

A data treatment more sensitive to changes in the Levich slope involves plotting $i_L/\omega^{1/2}$ vs. $\omega^{1/2}$.[34] Figure 7 presents these plots which also include more data points taken at the critical slow rotation speeds. Again, no alteration in the slopes was observed. If the chemical follow-up reaction is fast, one can conclude that either one or more electrons are initially transferred. The second possibility is obviated by the n-value determinations described previously.

The limits of a "fast follow-up reaction" vis-a-vis a rotating disk have been treated by Adams and co-workers.[35] They found that rotation speeds between 50 and 3000 rpm were sufficient to allow the determination of first-order rate constants of from 0.3 to 100 s^{-1}.

We have measured assumed pseudo-first-order rate constants for the disappearance of HMB·$^+$ by computer controlled double potential step chronoamperometry. In this experiment, the potential is stepped from a value where HMB is electroinactive (1.0 V) to a value well on the diffusion-limited plateau (1.6 V), and then back to the initial potential. The anodic current resulting from the oxidation of HMB to HMB·$^+$ is then compared to the cathodic current resulting from the reduction of HMB·$^+$ back to HMB.[36]

Typical double potential step current-time transients show that, on going from the melt to the melt plus varying amounts of benzene, the current due to HMB·$^+$ reduction to HMB increases. This is consonant with cyclic voltammetric data at high sweep rates. Computer calculated pseudo-first-order rate constants for HMB·$^+$ disappearance and the corresponding half-lives are tabulated in Table IV as a function of added

Table V. Collection Efficiencies[a] of Ring for $HMB^{\cdot+}$ Electrogenerated at the Disk

	$HMB^{\cdot+}$	
ω, rpm	Melt	50–50 melt–benzene
500	0.3	1.3
1000	0.4	2.4
2000	0.4	4.4
4000	0.6	7.9
7000	0.8	10.0
9000	0.9	12.0

[a] Percentage of ring current to disk currenf normalized for the ideal collection efficiency of the RRDE.

benzene. These numbers fall within the range of rate constants for chemical follow-up reactions as determined by rotating-disk experiments.[35]

An attempt was made to study the dependence of proton generation on $HMB^{\cdot+}$ disappearance using a rotating ring-disk electrode. If the chemical follow-up reaction is a deprotonation, then at high rotation rates $HMB^{\cdot+}$ generated at the disk should (prior to deprotonation) afford large currents when reduced at the ring. Conversely, at low rotation rates, little or no $HMB^{\cdot+}$ should survive in transit to the ring and large currents due to proton reduction would be observed. Unfortunately, on the vitreous carbon ring, proton reduction occurs very near to aluminum deposition and no reliable data were acquired. Figure 8 compares disk currents for the generation of $HMB^{\cdot+}$ to ring currents for the reduction of same at varying rotation speeds in both solvents. Table V presents the measured collection efficiencies for the ring for $HMB^{\cdot+}$ reduction. Again, in the melt plus benzene, a greater amount of cation radical survives to be reduced at the ring.

The results of the double potential step experiments in conjunction with rotating disk data show that a simple ECE mechanism cannot apply to the electrooxidation of HMB to PMB and DPM. On the basis of these data, we believe that $HMB^{\cdot+}$ is formed and a second intermediate "x", still at the one-electron stage, then follows. While we have no direct evidence for the structure of this intermediate, we speculate that it is a dimeric dication, IV.

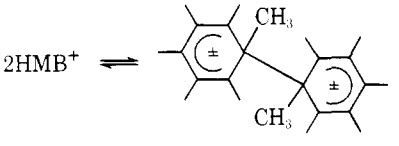

(12)

IV

Such a reaction has much precedent in aromatic oxidations[37] and the dication (a one-electron/HMB product) might have sufficient stability in the acidic melt to be metastable (1 s < $t_{1/2}$ < 10 min). Alternatives are the pentamethylbenzyl radical (V) and radical VI. We do not see, however, why these would

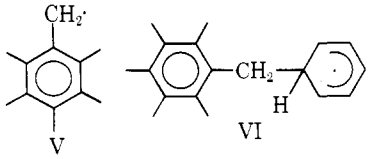

V VI

survive without being oxidized, abstracting a hydrogen, or dimerizing. If the dimeric dication were involved, it is predicted that $HMB^{\cdot+}$ would disappear in a second-order reaction. Thus, as a melt/HMB solution is diluted with benzene, $HMB^{\cdot+}$ should manifest longer half-lives. This is clearly borne out by the data in Table IV. Though the calculated pseudo-first-order rate constants may not reflect reality, they are phenomenologically indicative of greater $HMB^{\cdot+}$ stability in more dilute solutions.

Summary

The preparation of a novel high Lewis-acid room-temperature molten salt has been reported. Either tungsten or vitreous carbon is a suitable working electrode material in this solvent. The electrochemistry of several alkylaromatic hydrocarbons has been probed in the melt and in the melt plus benzene. Both media stabilize electrogenerated hexamethylbenzene cation radical as evidenced by cyclic voltammetry, rotating-ring disk experiments, and computer-controlled double potential step chronoamperometry. Preparative oxidations of hexamethylbenzene (HMB) in the melt plus benzene gave pentamethylbenzene (PMB) and diphenylmethane (DPM) in high yields. Subsequent oxidation of a reaction product, PMB, gave tetramethylbenzenes and more DPM. The source of the central methylene group in DPM is HMB leaving PMB. The phenyl groups of DPM arise from the benzene co-solvent.

Acknowledgment. We wish to thank Drs. J. H. Christie and J. Phillips for their technical assistance and helpful discussions of the results. This work was supported by the U.S. Army Research Office (Durham) under Grant DA-ARO-D-31-124-73-G18.

References and Notes

(1) Presented in part at the Mile High Electrochemistry Symposium, Rocky Mountain Section Electrochemical Society Meeting, May 3, 1975.
(2) Author to whom correspondence should be addressed.
(3) M. Fleischmann and D. Pletcher, *J. Electroanal. Chem.*, **25**, 449 (1970).
(4) H. L. Jones, L. G. Boxall, and R. A. Osteryoung, *J. Electroanal. Chem.*, **38**, 476 (1972).
(5) K. W. Fung, J. Q. Chambers and G. Mamantov, *J. Electroanal. Chem.*, **47**, 81 (1973).
(6) H. L. Jones and R. A. Osteryoung, *J. Electroanal. Chem.*, **38**, 476 (1974).
(7) V. R. Koch, L. L. Miller, and R. A. Osteryoung, *J. Org. Chem.*, **39**, 2416 (1974).
(8) D. E. Bartak and R. A. Osteryoung, *J. Electrochem. Soc.*, **122**, 600 (1975).
(9) H. L. Jones and R. A. Osteryoung, *Adv. Molten Salt Chem.*, **3**, 121–176 (1975).
(10) C. G. Swain, A. Ohno, D. K. Roe, R. Brown, and T. Maugh, II, *J. Am. Chem. Soc.*, **89**, 2648 (1967).
(11) W. T. Ford, R. J. Hauri, and D. J. Hart, *J. Org. Chem.*, **38**, 3916 (1973).
(12) D. D. Axtell, B. W. Good, W. W. Porterfield, and J. T. Yoke, *J. Am. Chem. Soc.*, **94**, 4555 (1972).
(13) K. Ziegler and O. W. Steudel, *Justus Liebigs Ann. Chem.*, **652**, 1 (1962).
(14) F. H. Hurley and T. P. Wier, Jr., *J. Electrochem. Soc.*, **98**, 203 (1951).
(15) H. L. Chum, V. R. Koch, L. L. Miller, and R. A. Osteryoung, *J. Am. Chem. Soc.*, **97**, 3264 (1975).
(16) "Glove Box Operations Manual", Vacuum Atmospheres Corp., North Hollywood, Calif., 1970, p 6.
(17) A. C. Vogel, "A Textbook of Practical Organic Chemistry", Longmans, Green and Co., London, 1966, p 173.
(18) J. Vedel and B. Tremillon, *Bull. Soc. Chim. Fr.*, 220 (1966).
(19) L. G. Boxall, H. L. Jones, and R. A. Osteryoung, *J. Electrochem. Soc.*, **121**, 212 (1974).
(20) It is important to maintain the temperature of the melt below 100 °C by adjusting the rate at which the aluminum chloride is added. Otherwise, a murky brown solution, difficult to purify, is produced.
(21) N. K. Gupta, *Rev. Sci. Instrum.*, **42**, 1368 (1971).
(22) E. P. Parry and R. A. Osteryoung, *Anal. Chem.*, **36**, 1360 (1964).
(23) J. Phillips, R. J. Gale, R. Wier, and R. A. Osteryoung, *Anal. Chem.*, **48**, 1266 (1976).
(24) D. T. Napp, D. C. Johnson, and S. Bruckenstein, *Anal. Chem.*, **39**, 481 (1967).
(25) L. Byrd, L. L. Miller, and D. Pletcher, *Tetrahedron Lett.*, 2419 (1972).
(26) U. Svanholm and V. D. Parker, *Tetrahedron Lett.*, 471 (1972).
(27) L. Eberson and K. Nyberg, *Acc. Chem. Res.*, **6**, 106 (1973).
(28) K. Nyberg, *Acta Chem. Scand.*, **25**, 2499 (1971).
(29) K. Nyberg, *Acta Chem. Scand.*, 1609 (1970).
(30) G. Olah, "Friedel–Crafts and Related Reactions", Vol. 1, G. Olah, Ed., Interscience, New York, N.Y., 1963, pp 36–38.
(31) P. S. Hofman, D. J. Reiding, and W. T. Nauta, *Recl. Trav. Chim. Pays-Bas*, **79**, 790 (1960).
(32) A. Streitwieser Jr. and L. Reif, *J. Am. Chem. Soc.*, **86**, 1988 (1964).
(33) K. Nyberg and A. Trojánek, *Collect. Czech. Chem. Commun.*, **40**, 526 (1975).
(34) L. S. Marcoux, J. M. Fritsch, and R. N. Adams, *J. Am. Chem. Soc.* **89**, 5766 (1967).
(35) P. A. Malachesky, L. S. Marcoux, and R. N. Adams, *J. Phys. Chem.*, **70**, 4068 (1966).
(36) W. M. Schwarz and I. Shain, *J. Phys. Chem.*, **69**, 30 (1965).
(37) A. Ronlán, O. Hammerlich, and V. D. Parker, *J. Am. Chem. Soc.*, **95**, 7132 (1973), and references cited therein.